



## High Impulsivity Predicts the Switch to Compulsive Cocaine-Taking

David Belin *et al.*

*Science* **320**, 1352 (2008);

DOI: 10.1126/science.1158136

*This copy is for your personal, non-commercial use only.*

If you wish to distribute this article to others, you can order high-quality copies for your colleagues, clients, or customers by [clicking here](#).

Permission to republish or repurpose articles or portions of articles can be obtained by following the guidelines [here](#).

**The following resources related to this article are available online at [www.sciencemag.org](http://www.sciencemag.org) (this information is current as of April 24, 2013):**

**Updated information and services**, including high-resolution figures, can be found in the online version of this article at:

<http://www.sciencemag.org/content/320/5881/1352.full.html>

**Supporting Online Material** can be found at:

<http://www.sciencemag.org/content/suppl/2008/06/05/320.5881.1352.DC1.html>

<http://www.sciencemag.org/content/suppl/2008/06/13/320.5881.1352.DC2.html>

This article **cites 27 articles**, 6 of which can be accessed free:

<http://www.sciencemag.org/content/320/5881/1352.full.html#ref-list-1>

This article has been **cited by** 71 article(s) on the ISI Web of Science

This article has been **cited by** 25 articles hosted by HighWire Press; see:

<http://www.sciencemag.org/content/320/5881/1352.full.html#related-urls>

This article appears in the following **subject collections**:

Neuroscience

<http://www.sciencemag.org/cgi/collection/neuroscience>

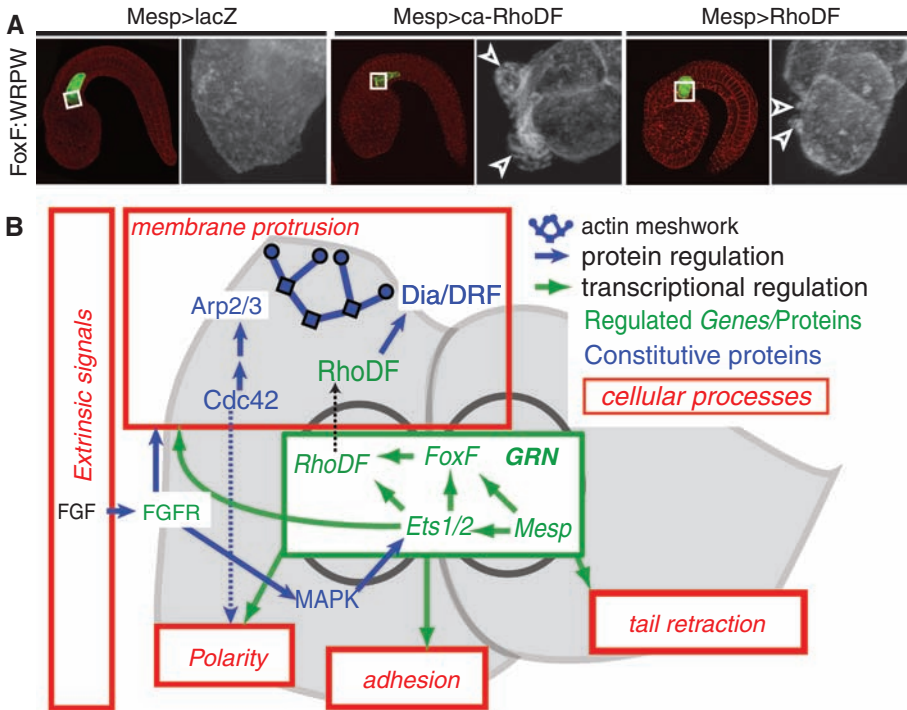


**Fig. 4.** RhoDF induces membrane protrusion in nonmigrating cells. **(A)** B7.5-lineage cells coexpressing FoxF:WRPW and lacZ, ca-RhoDF, or RhoDF. [Whole embryos and close-up views (boxes) are shown. Red indicates Alexa-phalloidin counterstaining.] Arrowheads indicate protrusions. **(B)** Summary model. The gene regulatory network (GRN) influences polarity, adhesion, tail retraction, and membrane protrusion. Membrane protrusion is controlled in part by FoxF- and Ets1/2-mediated upregulation of RhoDF, which functions together with constitutively expressed Cdc42, Dia/DRF (blue circles), and Arp2/3 (blue squares).

inputs, stressing the fact that RhoDF-induced protrusive activity is regulated by multiple inputs from the heart specification network (Fig. 4B and figs. S10 to S12). A separate enhancer controls *RhoDF* expression in the notochord (fig. S11). In principle, this modular organization of the *RhoDF* cis-regulatory elements permits activation by distinct gene regulatory networks in the notochord and TVCs. RhoDF contributes to the formation of protrusions in migrating TVCs and probably also in intercalating notochord cells (Fig. 3B and fig. S14). Unlike TVCs, notochord cells maintain adhesive contacts with their neighbors. In *laminin- $\alpha$ 3/4/5* mutants, these adhesive contacts are disrupted and notochord cells migrate away from their normal location, displaying dynamic protrusions reminiscent of those induced by ca-RhoDF (22) (fig. S15). Thus, the notochord and TVCs deploy different suites of shared (such as protrusions) and tissue-specific (such as adhesive properties) cellular modules. We propose that tissue-specific gene networks control the distinct combinations of cellular modules underlying the morphogenetic diversity observed during evolution and development.

**References and Notes**

1. A. Stathopoulos, M. Levine, *Dev. Cell* **9**, 449 (2005).
2. E. H. Davidson *et al.*, *Science* **295**, 1669 (2002).
3. K. S. Imai, M. Levine, N. Satoh, Y. Satou, *Science* **312**, 1183 (2006).
4. C. Bakal, J. Aach, G. Church, N. Perrimon, *Science* **316**, 1753 (2007).

5. R. Zaidel-Bar, S. Itzkovitz, A. Ma'ayan, R. Iyengar, B. Geiger, *Nat. Cell Biol.* **9**, 858 (2007).
6. Y. Satou, K. S. Imai, N. Satoh, *Development* **131**, 2533 (2004).
7. B. Davidson, W. Shi, M. Levine, *Development* **132**, 4811 (2005).

8. B. Davidson, W. Shi, J. Beh, L. Christiaen, M. Levine, *Genes Dev.* **20**, 2728 (2006).
9. J. Beh, W. Shi, M. Levine, B. Davidson, L. Christiaen, *Development* **134**, 3297 (2007).
10. L. Borghese *et al.*, *Dev. Cell* **10**, 497 (2006).
11. X. Wang *et al.*, *Dev. Cell* **10**, 117 (2006).
12. S. A. Koestler, S. Auinger, M. Vinzenz, K. Rottner, J. V. Small, *Nat. Cell Biol.* **10**, 306 (2008).
13. C. Yang *et al.*, *PLoS Biol.* **5**, e317 (2007).
14. P. A. Randazzo, *Dev. Cell* **4**, 287 (2003).
15. S. Pellegrin, H. Mellor, *Curr. Biol.* **15**, 129 (2005).
16. J. C. Corbo, M. Levine, R. W. Zeller, *Development* **124**, 589 (1997).
17. K. A. Edwards, M. Demsky, R. A. Montague, N. Weymouth, D. P. Kiehart, *Dev. Biol.* **191**, 103 (1997).
18. S. Ellis, H. Mellor, *Curr. Biol.* **10**, 1387 (2000).
19. C. D. Nobes, A. Hall, *Cell* **81**, 53 (1995).
20. R. Rohatgi *et al.*, *Cell* **97**, 221 (1999).
21. L. Ma, R. Rohatgi, M. W. Kirschner, *Proc. Natl. Acad. Sci. U.S.A.* **95**, 15362 (1998).
22. M. T. Veeman *et al.*, *Development* **135**, 33 (2007).
23. Microarray data available at ArrayExpress; accession number, E-MEXP-1478. We thank J. Beh, A. Philips, and P. Lemaire for sharing constructs; M. Blanchette and V. Peng for help with microarrays; Y. Satou for expressed sequence tag sequences and annotations; and W. Shi, K. Imai, and U. Rothbacher for help with microinjections. Authors' contributions were as follows: L.C. designed the project, performed and analyzed experiments, and prepared the figures; B.D. and T.K. designed the custom microarray; L.C. and W.P. performed in situ hybridizations; L.C. and H.N. performed the FACS experiments; L.C. and K.V. analyzed the microarray data; and L.C. and M.L. wrote the paper. This work was funded by NSF grant IOB 0445470 and NIH grant 18B-106681 to M.L., a grant from the Gordon and Betty Moore Foundation to the Center for Integrative Genomics, and an American Heart Association fellowship (0625042Y) to B.D.

**Supporting Online Material**

www.sciencemag.org/cgi/content/full/320/5881/1349/DC1  
 Materials and Methods  
 SOM Text  
 Figs. S1 to S16  
 Tables S1 and S2  
 References  
 21 March 2008; accepted 9 May 2008  
 10.1126/science.1158170

# High Impulsivity Predicts the Switch to Compulsive Cocaine-Taking

David Belin,<sup>1\*</sup> Adam C. Mar,<sup>1</sup> Jeffrey W. Dalley,<sup>1,2</sup> Trevor W. Robbins,<sup>1</sup> Barry J. Everitt<sup>1\*</sup>

Both impulsivity and novelty-seeking have been suggested to be behavioral markers of the propensity to take addictive drugs. However, their relevance for the vulnerability to compulsively seek and take drugs, which is a hallmark feature of addiction, is unknown. We report here that, whereas high reactivity to novelty predicts the propensity to initiate cocaine self-administration, high impulsivity predicts the development of addiction-like behavior in rats, including persistent or compulsive drug-taking in the face of aversive outcomes. This study shows experimental evidence that a shift from impulsivity to compulsivity occurs during the development of addictive behavior, which provides insights into the genesis and neural mechanisms of drug addiction.

Compulsive cocaine use has been hypothesized to result from a failure in top-down executive control over maladaptive habit learning (1, 2). In neural terms, this may reflect the diminishing influence of prefrontal cortical function, as behavioral control devolves from ventral to dorsal striatum (1). In behavioral terms, we predict that the development of addiction reflects a shift from impulsivity to compulsivity (3).

Human studies have implicated individual differences in different forms of impulsivity and sensation-seeking in vulnerability to drug use and abuse (4–6). However, whether the enhanced impulsivity observed in drug addicts (7, 8) predates the onset of compulsive drug use or is a consequence of protracted exposure to drugs has not been fully established. In addressing this issue experimentally, we operationalized these human traits in

experimental animals as an inability to wait before performing an appropriate response, one phenotype of impulsivity (9) measured as premature responses in a five-choice serial reaction-time task (5-CSRTT) of sustained visual attention (10), as distinct from locomotor reactivity to a novel environment, a sensation-seeking phenotype (11). These animal models support the existence of a “vulnerable phenotype” that predisposes to drug addiction. Thus, outbred rats exhibiting high levels of novelty-induced locomotor activity, called high

<sup>1</sup>Behavioural and Clinical Neuroscience Institute and Department of Experimental Psychology, University of Cambridge, Downing Street, Cambridge CB2 3EB, UK. <sup>2</sup>Department of Psychiatry, University of Cambridge, Addenbrooke’s Hospital, Hills Road, Cambridge CB2 2QQ, UK.

\*To whom correspondence should be addressed. E-mail: bdb26@cam.ac.uk (D.B.); bje10@cam.ac.uk (B.J.E.)

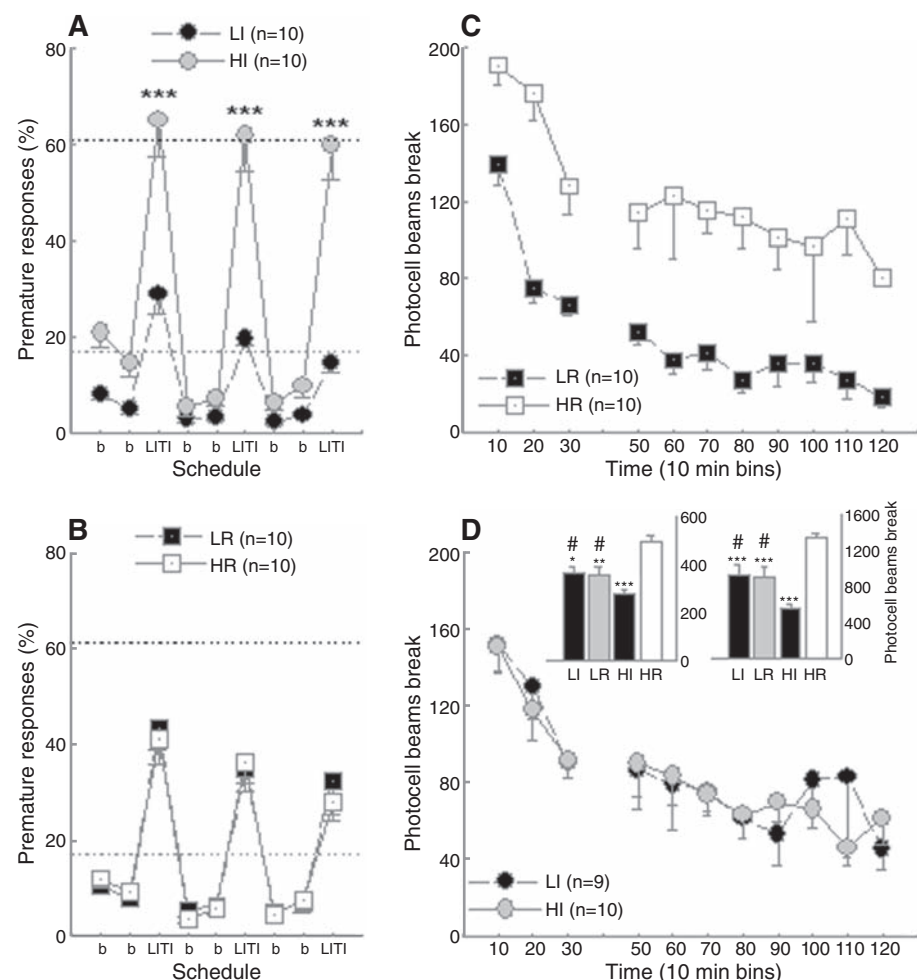


**Fig. 1.** Impulsivity and novelty-induced locomotor activity: two distinct phenotypes. On two baseline days (b), premature responses in the 5-CSRTT were measured. **(A and B)** During long intertrial intervals (LITIs), HI rats showed more premature responses than LI rats (Group:  $F_{3,36} = 14.4$ ,  $P < 0.01$ ; Schedule:  $F_{8,288} = 130.22$ ,  $P < 0.01$ ; Schedule  $\times$  Group:  $F_{24,288} = 7.01$ ,  $P < 0.01$ ) (\*\* $P < 0.001$ ) (A) and HR ( $P < 0.01$ ) or LR rats ( $P < 0.05$ ) (B). HR rats did not differ from LR rats or from LI subjects (B). **(C and D)** HR rats were more reactive to novelty than LR rats for the first 30 min (left histogram, inset) or the total duration of the session (right histogram) (Group:  $F_{3,35} = 12.17$ ,  $P < 0.01$  and  $F_{3,35} = 17.63$ ,  $P < 0.01$ , respectively; Group  $\times$  Time:  $F_{6,70} = 1.26$ , not significant, and  $F_{30,350} < 1$ ,  $P < 0.001$ , respectively). (Inset) HI and LI subjects differed from both HR ( $P < 0.01$ ) and LR rats ( $\#$ ,  $P < 0.01$ ) but never from each other. \*Comparison with HR: \* $P < 0.05$ , \*\* $P < 0.01$ , \*\*\* $P < 0.001$ . (D) Black and gray dotted lines represent the average premature responses during the last two long intertrial intervals for HI and LI rats, respectively.

responder (HR), show increased sensitivity to the reinforcing effects of addictive drugs and self-administer lower doses of psychostimulants than low-responder (LR) littermates (11). Impulsivity, on the other hand, correlates with ethanol intake (12) and predicts instead the escalation of cocaine self-administration (10, 13), which may be more indicative of a necessary stage in the transition to compulsive drug-seeking. Although these studies have addressed the initiation of drug-taking, they have not captured the essential feature of addiction, namely, the persistence of drug-seeking in the face of negative consequences, a characteristic incorporated into recent animal models based on the DSM-IV criteria for substance dependence (14, 15). Therefore, we have used a model of addiction based on individual differences in compulsive cocaine use (14) to investigate the contrasting

contribution of high impulsivity (HI) and high reactivity to novelty (HR) to the development of compulsive drug-taking.

In this model, we have operationally defined three addiction-like criteria in rats that correspond to those of the DSM-IV description of substance dependence (16), namely, (i) increased motivation to take the drug, (ii) an inability to refrain from drug-seeking, and (iii) maintained drug use despite aversive consequences [see (17) for details]. Thus, rats positive for none of the three criteria (zero-criteria rats) are resistant to addiction, whereas rats that have three addiction-like criteria (three-criteria rats) are considered “addicted,” and represent 15 to 20% of the population initially exposed to cocaine (14), a proportion that is similar to that observed in human populations (18).

To compare the propensity of HI and HR rats both to acquire cocaine self-administration and to make the transition to compulsive cocaine-taking, we first identified HI and LI rats in the 5-CSRTT (10), then HR and LR rats in a novelty-induced locomotor activity procedure (11). Subsequently, we compared the propensity of these different groups to acquire cocaine self-administration and to develop the three addiction-like criteria following protracted self-administration (17). HI and LI rats did not differ in their novelty-induced locomotor activity; conversely, HR and LR rats were not impulsive (Fig. 1, A and B). As predicted (11), HR rats were more prone to acquire cocaine self-administration than LR rats, showing an upward shift in the cocaine dose-response curve (Fig. 2). However, HI rats did not differ from LI rats in their acquisition of cocaine self-administration.

After 40 days of cocaine self-administration, we measured the three addiction-like behaviors in a cohort of 23 rats (17), so that each rat was defined as showing none or one, two, or three of these behaviors (table S2), as well as an addiction score, calculated as the sum of the standardized

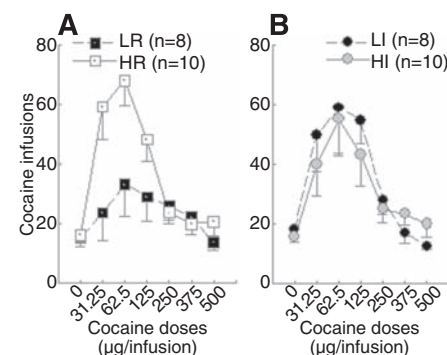


**Fig. 2.** Novelty-induced locomotor activity predicts the propensity to acquire cocaine self-administration. **(A)** HR rats showed an upward shift of the cocaine dose-response curve compared with LR littermates (Group:  $F_{1,16} = 4.9$ ,  $P < 0.05$ ; Dose:  $F_{6,96} = 11.73$ ,  $P < 0.01$ ; and Group  $\times$  Dose:  $F_{6,96} = 4.39$ ,  $P < 0.01$ ). HR rats infused more cocaine at the lowest three doses than vehicle ( $P < 0.01$ ). **(B)** HI and LI subjects did not differ in their number of self-administered cocaine infusions (Group:  $F_{1,16} < 1$ ; Dose:  $F_{6,96} = 10.79$ ,  $P < 0.01$ ; Group  $\times$  Dose:  $F_{6,96} < 1$ ).

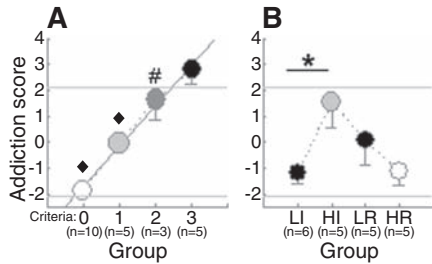


**Fig. 3.** HI rats closely resemble three-criteria rats. After protracted self-administration, rats with zero, one, two, or three criteria were identified. **(A)** When ranked on a linear addiction scale ( $R^2 = 0.99$ , Group:  $F_{3,19} = 34.43$ ,  $P < 0.01$ ), three-criteria rats had addiction scores ( $2.8 \pm 0.6$ ) above the standard deviation (2.1), and higher than all the other groups (versus zero- and one-criteria rats:  $\blacklozenge$ ,  $P < 0.01$ , versus 2-criteria rats:  $\#$ ,  $P \leq 0.05$ ). **(B)** HI rats displayed higher addiction scores than LI rats ( $F_{1,9} = 7.55$ ,  $*P < 0.05$ ), whereas HR rats did not differ from LR rats. Only HI rats did not differ from three-criteria rats for their addiction score ( $F_{5,30} = 10.13$ ,  $P < 0.01$ ) and displayed higher addiction scores than zero-criteria ( $P < 0.01$ ) and HR rats ( $P < 0.05$ ). HR, LR, and LI rats did not differ from zero-criteria rats.

scores of each of the addiction-like criteria (17). Thus, rats with zero, one, two, or three criteria were linearly distributed along an addiction scale, corresponding operationally to the Addiction Severity Index (ASI) in humans (17, 19). On this scale, three-criteria rats had scores higher than all the other groups (Fig. 3A), especially when compared with zero-criteria animals, from which they differed for each of the addiction-like behaviors (fig. S1). Only the zero-criteria rats had highly negative addiction scores.

Although reactivity to novelty predicts the vulnerability to acquire cocaine self-administration, it is high impulsivity that predicts the transition from controlled to compulsive cocaine-taking. HI rats displayed higher addiction scores than LI rats whereas, in marked contrast, HR rats did not differ from LR rats (Fig. 3B). LI, HR, and LR rats were represented mainly in the zero- and one-criteria populations; however, HI rats were largely represented in the two- and three-criteria populations. Additionally, only HI rats were more frequently represented in the three-criteria group than in the zero-criteria group (table S1).

A factor analysis revealed that impulsivity and addiction-like behavior are explained by the same factor that was itself orthogonal to reactivity to novelty, thereby identifying an impulsivity-addiction construct (fig. S2). Thus, HI rats did not differ from three-criteria rats in any of their addiction-like behaviors (Fig. 4A and fig. S3).

More specifically, the high addiction score of HI rats derived from the development of compulsive cocaine self-administration. HI rats displayed greater resistance to punishment of the drug-taking response than did LI, HR, and LR rats (Fig. 4A), and at the population level, correlational analysis revealed that impulsivity predicts compulsivity (Fig. 4B). However, HI rats did not differ from

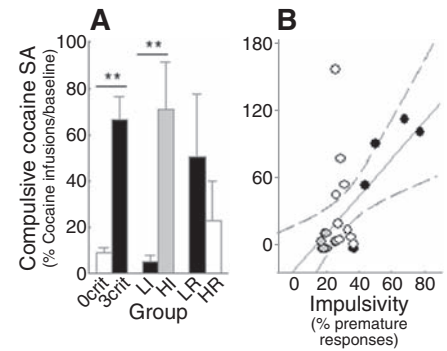
**Fig. 4.** Impulsivity predicts the transition to compulsivity. **(A)** HI rats receiving punishment (17) continued compulsive cocaine self-administration (SA). HI rats ( $n = 5$ ) displayed higher resistance to punishment than LI rats ( $n = 6$ ) ( $F_{1,9} = 12.79$ ,  $P < 0.01$ ), whereas HR ( $n = 5$ ) rats did not differ from LR rats ( $n = 5$ ). When compared with zero- and three-criteria rats for their resistance to punishment (Group:  $F_{5,30} = 10.13$ ,  $P < 0.01$ ), only HI rats were similar to three-criteria rats; they showed greater resistance to punishment than zero-criteria, LI, and HR rats ( $P < 0.05$ ). LI and HR rats differed from three-criteria, but not from zero-criteria, rats (A).  $**P < 0.01$ . **(B)** Impulsivity predicts compulsive cocaine self-administration ( $R = 0.42$ ,  $P < 0.05$ ). Gray and black shadings represent LI and HI rats, respectively.

LI, HR, or LR rats in their total intake of cocaine (fig. S3); therefore, the development of compulsive cocaine-taking observed specifically in the highly impulsive rats cannot be attributed to differential exposure to cocaine. Because clinical investigations generally compare addicted subjects with drug-naïve controls, we analyzed whether animals vulnerable and resistant to addiction differed in their impulsivity and locomotor reactivity to novelty before any exposure to cocaine. This analysis showed that three-criteria rats were more impulsive, but not more reactive to novelty, than zero-criteria rats before cocaine self-administration (fig. S4).

These data allow us to identify one variety of impulsivity, measured as an inability to wait and sample predictive stimuli before responding (20), as a key behavioral marker specific for the vulnerability to progress to compulsive cocaine use, the hallmark of addiction. Our results are in accord with observations that (i) highly impulsive humans are overrepresented in drug-addicted populations (21), (ii) impulsivity or sensation-seeking may predate compulsive drug use (22, 23), and (iii) there is a high comorbidity between drug addiction and disorders characterized by impulsive behavior, such as attention deficit-hyperactivity disorder (ADHD) (21).

The results indicate that the relation between high impulsivity and addiction-like behavior is completely independent of the initial propensity to acquire cocaine self-administration (fig. S2) (17), an observation consistent with the demonstration that impulsivity is unrelated to the subjective effects of oral amphetamine administration (24). Instead, this early vulnerability to cocaine's reinforcing effects was predicted by high locomotor reactivity to novelty. Our observations further suggest that the subjective and behavioral responses to cocaine during initial exposure to the drug do not determine the subsequent progression to addiction, as might perhaps have been previously suspected (11).

Our study also provides experimental evidence that high levels of impulsivity can antedate the onset of compulsive drug use and, thereby, emphasizes the importance of preexisting impulsivity observed in addicts (2, 4, 7). Moreover, by demonstrating the link between impulsivity and compulsivity in the development of addiction, these data provide a major impetus for investigating the neurobiological mechanisms underlying this transition. One candi-



date is the apparent devolution of control over drug-seeking behavior from the ventral to the dorsal striatum (25), which has been shown to depend on the cascading, serial ascending circuitry that links these striatal domains via its regulatory dopaminergic innervation arising in the midbrain (26, 27). This hypothesis is further supported by the observation that the early vulnerability to escalate cocaine intake shown by highly impulsive rats is predicted by low D2 and/or D3 dopamine receptor levels in the ventral, but not the dorsal, striatum (10). In contrast, chronic exposure to cocaine in monkeys (28) and drug-abusers (29) is associated with low D2 and/or D3 dopamine receptor availability, predominantly in the dorsal striatum.

#### References and Notes

- B. J. Everitt, T. W. Robbins, *Nat. Neurosci.* **8**, 1481 (2005).
- J. D. Jentsch, J. R. Taylor, *Psychopharmacology (Berlin)* **146**, 373 (1999).
- G. F. Koob, M. Le Moal, *Neuropsychopharmacology* **24**, 97 (2001).
- M. J. Kreek, D. A. Nielsen, E. R. Butelman, K. S. LaForge, *Nat. Neurosci.* **8**, 1450 (2005).
- N. Chakroun, J. Doron, J. Swendsen, *Encephale* **30**, 564 (2004).
- T. A. Wills, D. Vaccaro, G. McNamara, *J. Subst. Abuse* **6**, 1 (1994).
- G. Dom, P. D'Haene, W. Hulstijn, B. Sabbe, *Addiction* **101**, 50 (2006).
- M. L. Zilberman, H. Tavares, D. C. Hodgins, N. el-Guebaly, *J. Addict. Dis.* **26**, 79 (2007).
- J. L. Evenden, *Psychopharmacology (Berlin)* **146**, 348 (1999).
- J. W. Dalley et al., *Science* **315**, 1267 (2007).
- P. V. Piazza, J. M. Deminiere, M. Le Moal, H. Simon, *Science* **245**, 1511 (1989).
- C. X. Poulos, A. D. Le, J. L. Parker, *Behav. Pharmacol.* **6**, 810 (1995).
- J. L. Perry, E. B. Larson, J. P. German, G. J. Madden, M. E. Carroll, *Psychopharmacology (Berlin)* **178**, 193 (2005).
- V. Deroche-Gamonet, D. Belin, P. V. Piazza, *Science* **305**, 1014 (2004).
- L. J. Vanderschuren, B. J. Everitt, *Science* **305**, 1017 (2004).
- American Psychiatric Association, *Diagnostic and Statistical Manual of Mental Disorders: DSM-IV-TR* (American Psychiatric Association, Washington, DC, ed. 4, text revised, 2000).
- Materials and methods are available as supporting material on Science Online.
- J. C. Anthony, L. A. Warner, R. C. Kessler, *Exp. Clin. Psychopharmacol.* **2**, 244 (1994).
- S. H. Rikoon, J. S. Cacciola, D. Carise, A. I. Alterman, A. T. McLellan, *J. Subst. Abuse Treat.* **31**, 17 (2006).
- J. Evenden, *Psychopharmacology (Berlin)* **143**, 111 (1999).
- J. T. Nigg et al., *J. Am. Acad. Child Adolesc. Psychiatry* **45**, 468 (2006).
- S. Dawe, N. J. Loxton, *Neurosci. Biobehav. Rev.* **28**, 343 (2004).

23. K. J. Sher, B. D. Bartholow, M. D. Wood, *J. Consult. Clin. Psychol.* **68**, 818 (2000).
24. T. L. White, D. C. Lott, H. de Wit, *Neuropsychopharmacology* **31**, 1064 (2006).
25. L. J. Vanderschuren, P. Di Ciano, B. J. Everitt, *J. Neurosci.* **25**, 8665 (2005).
26. D. Belin, B. J. Everitt, *Neuron* **57**, 432 (2008).
27. S. N. Haber, J. L. Fudge, N. R. McFarland, *J. Neurosci.* **20**, 2369 (2000).
28. M. A. Nader *et al.*, *Nat. Neurosci.* **9**, 1050 (2006).
29. N. D. Volkow *et al.*, *Synapse* **14**, 169 (1993).
30. This work has been supported by grants from the Foundation Fyssen to D.B. and the U.K. Medical Research Council (MRC) no. G9536855 to B.J.E. and was completed within the Behavioural and Clinical Neuroscience Institute, which is supported by a joint grant from the MRC and the Wellcome Trust. The authors thank D. Theobald for his assistance and M. Solinas and A. Rauscent for their comments on this manuscript. Behavioral experiments and statistical analyses were designed and performed by D.B. The manuscript was prepared by D.B., A.C.M., J.W.D., T.W.R., and B.J.E. The authors declare that they have no competing financial interests.

### Supporting Online Material

www.sciencemag.org/cgi/content/full/320/5881/1352/DC1  
Materials and Methods  
SOM Text  
Figs. S1 to S4  
Tables S1 and S2  
References

21 March 2008; accepted 7 May 2008  
10.1126/science.1158136

# Patches with Links: A Unified System for Processing Faces in the Macaque Temporal Lobe

Sebastian Moeller, Winrich A. Freiwald, Doris Y. Tsao\*

The brain processes objects through a series of regions along the ventral visual pathway, but the circuitry subserving the analysis of specific complex forms remains unknown. One complex form category, faces, selectively activates six patches of cortex in the macaque ventral pathway. To identify the connectivity of these face patches, we used electrical microstimulation combined with simultaneous functional magnetic resonance imaging. Stimulation of each of four targeted face patches produced strong activation, specifically within a subset of the other face patches. Stimulation outside the face patches produced an activation pattern that spared the face patches. These results suggest that the face patches form a strongly and specifically interconnected hierarchical network.

An essential step to understand the neural mechanism underlying any percept is to identify its anatomical substrate. For example, many theoretical models of object recognition propose a hierarchical architecture (1, 2), but it remains unclear if and how such hierarchical models are actually implemented by the brain.

The face-processing system of macaque monkeys provides an ideal preparation for dissecting the large-scale functional anatomy of object recognition. Almost all macaques have a set of face-selective regions that can be easily identified by functional magnetic resonance imaging (fMRI) (3, 4) and readily targeted for anatomical experiments (5). Understanding the connectivity of these regions should provide insights into the large-scale circuitry used by the brain to perceive a complex form.

It is debated whether face processing relies on a sequence of dedicated processing stages (6) or whether it relies on distributed representations (7). The former model predicts that face-selective regions show strong connections to each other but not to surrounding non-face selective temporal cortex, whereas the latter predicts strong connections between face-selective regions and surrounding non-face selective temporal cortex (8).

Tracer injections made into the macaque temporal lobe reveal a patchy connectivity pattern (9–14). For example, Saleem *et al.* found that

injections into TEO (a cytoarchitectonic area in posterior inferior temporal cortex) produce labeling in TE (a cytoarchitectonic area in anterior temporal cortex) in two to five discrete foci (10). However, the functional properties of cells at injection and termination sites were not identified in these studies. In general, to dissect functional anatomy, it is necessary to combine connectivity maps with functional topography (15, 16). Specifically, the connections of the macaque face patches cannot be deduced from previous studies. To identify the anatomical connections of the macaque face patches, we used fMRI-guided electrical microstimulation combined with simultaneous fMRI (17–19).

Macaque monkeys typically have six discrete, bilateral patches of face-selective cortex (Fig. 1 and fig. S1). These patches are organized as follows: one posterior patch on the lateral surface of area TEO (which we will refer to as “PL,” for posterior lateral); two middle face patches in posterior area TE, one located in the fundus of the superior temporal sulcus (STS) (“MF,” for middle fundus) and one on the lower lip of the STS (“ML,” for middle lateral); and three patches in anterior area TE, one located near the fundus of the STS (“AF,” for anterior fundus), one on the lower lip of the STS and adjacent gyrus, in area TEad (“AL,” for anterior lateral), and one more medially on the ventral surface, just lateral and anterior to the anterior middle temporal sulcus (AMTS), in area TEav (“AM,” for anterior medial) (20).

We identified the locations of face patches in four monkeys (M1 through M4) by scanning them with a standard face-localizer stimulus (3). Individual animals and hemispheres exhibited slight

variations on the prototypical pattern just described. Face patches in the left and right hemispheres of monkey M1 on flattened maps of the posterior two-thirds of the brain excluding prefrontal cortex and in coronal slices are shown in Fig. 1, A and B; this animal had five discrete face regions in the right hemisphere (PL and ML were confluent). Time courses from the face patches confirm the face selectivity of each patch (Fig. 1C). The face patches of the three other animals (M2 through M4) used in this study are shown in fig. S1.

We then targeted a subset of the face patches for microstimulation combined with simultaneous fMRI. We first verified that the electrode correctly targeted each face patch by recording spiking activity. We then transferred the animal to the scanner for microstimulation. We stimulated a total of four different face patches (ML, AL, AM, and AF); several inferotemporal sites neighboring the face patches; and a site in the upper bank of the STS (table S1).

We first targeted ML in monkey M1. Magnetic resonance images of the electrode descending into ML, in sagittal and coronal planes, are shown in Fig. 2A. The response profile of the last cell recorded from this patch before microstimulation is shown in Fig. 2B; this cell was highly face selective (as were neighboring ones above it). The location of the electrode tip, marked on the flat map, confirms that stimulation was within ML (Fig. 2C). Comparing activation with and without microstimulation revealed five discrete regions in the temporal lobe (Fig. 2C). Stimulation resulted in a large spread around the electrode tip, a stretch of 4 mm with little activity, and then three discrete anterior patches located 6 to 11 mm anterior to the stimulation site. These patches coincided with the three anterior face patches of this monkey (compare Fig. 1A with Fig. 2C, and Fig. 1B with Fig. 2D). This activation pattern was reproducible across scan sessions and was not sensitive to the choice of significance threshold (fig. S2). Time courses from the six face patches confirm strong activation during microstimulation epochs (Fig. 2E).

The results of stimulating ML in two additional animals (M2 and M3) are shown in fig. S3. In monkey M2, stimulation in ML elicited activation in three other face patches: MF, PL, and AL. In monkey M3, stimulation in ML elicited activation in two other face patches: PL and AL. Results from the three animals show that ML is strongly connected to PL and AL and more variably to the remaining face patches.

Institute for Brain Research and Center for Advanced Imaging, University of Bremen, Post Office Box 330440, D-28334 Bremen, Germany.

\*To whom correspondence should be addressed. E-mail: doris@nmr.mgh.harvard.edu